7.3 COMPOSITE BOW ECHO OBSERVED DURING BAMEX

D. Ahijevych*, G. Bryan, M. Weisman, S. Trier, C. Davis, and D. Dowell
National Center for Atmospheric Research, Boulder, Colorado

1 INTRODUCTION

During the Bow Echo and MCV Experiment of 2003 (Davis et al. 2003), warm season bow echoes were directly sampled over the central U.S. A Lear jet released several dozen dropsondes and mobile surface units released many rawinsondes ahead of, within and behind the convective lines. By combining these temperature, moisture, pressure and wind observations in a system-relative composite, we obtain a three-dimensional analysis of thermodynamic fields in a mature bow echo with unprecedented resolution. Both non-severe and severe bow echoes are included in this composite.

Sounding positions are remapped in terms of distance from the convective line along the bow echo path and distance right or left of the apex. The system motion vector is subtracted from the wind observations, and wind direction is relative to the system motion vector. The average thermodynamic profile ahead of each bow echo is subtracted from the observed soundings, so we are left with deviations from the environmental mean.

The structure of the composite bow echo is consistent with conclusions drawn from previous numerical modeling studies, such as the importance of low-level environmental wind shear perpendicular to the convective line (Rotunno et al., 1988) and an elevated rear inflow jet (Weisman, 1992). Distinctive aspects of the composite bow echo include its deep cold pool (4 km) and the double minimum in temperature perturbation in the vertical. Additionally, the environment ahead of the convective line exhibits a weak baroclinic zone with enhanced vertical wind shear along and slightly to the right of the system path.

2 METHODOLOGY

2.1 Dataset

We begin with the BaMEX sounding composite dataset provided by the EOL at NCAR. All available sounding platforms are combined and interpolated every 5-hPa. Most suspicious data are flagged by the automated procedure described in (JOSS, 2006), but a small fraction is flagged only after visual inspection. Bad and suspicious data are ignored.

To be included, a sounding must reside in the swath of a bow echo or in the undisturbed environment ahead of the convective line within 350 km of the apex. See Fig. 2 for an illustration of these criteria. After removing extraneous soundings, we are left with 137 dropsonde, 30 MGLASS, six national weather service (NWS), and one ARM profile.

We also include 204 hourly wind profiles from the NOAA profiler network (NPN; Weber et al., 1993). NPN data are only used if they pass all quality control checks described in FSL (2006) and are within 300 km of the bow echo apex. The hourly wind profiles have been produced from 6-min averages and we use the midpoint of the one-hour averaging window as the observation time.

2.2 Bow echo identification and tracking

To be considered a bow echo, the horizontal radar reflectivity pattern must exhibit a quasi-continuous convective line at least 20 km long and over 35 dBZ. In all, we sampled 19 different systems in this mature stage (Fig. 1). For the compositing method to be valid, we need steady-state conditions, so we ignore the growth and dissipation stages of the bow echo. The mature phases lasted from 1.5 to 7.75 h in our population, with a mean duration of 4.2 h.

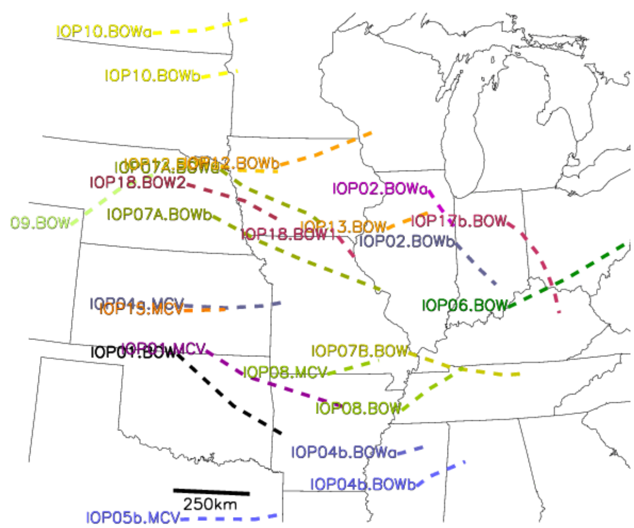

Fig. 1. Bow echo tracks from BAMEX following the path of the bow echo apex as observed in radar loops.

Bow echoes exhibit a variety of shapes and sizes (Przybylinski, 1995; Klimowski et al., 2004), but they also have common features tied to important physical processes. Our coordinate system is designed around this principle. In this spirit, the anchor of our coordinate system is the convective line. In a gross sense, this line

*Corresponding author: David Ahijevych
National Center for Atmospheric Research
Boulder, CO
Email: ahijevyc@ucar.edu

separates the bow echo downdraft from the large scale environment. It is the most objectively defined feature and identifiable by tracking a quasi-continuous arc-shaped segment of high reflectivity in radar loops.

2.2.1 Distance ahead of convective line

In our bow-echo relative coordinate system, the x-dimension is distance ahead of the convective line. It is measured parallel to the motion vector of the bow echo (at the time of sounding launch or the midpoint of the wind profiler's 1-h averaging window). Displacement ahead of the convective line is defined as positive and displacement behind the convective line is negative (Fig. 2).

2.2.2 Distance right or left of bow apex track

The y–dimension is distance measured perpendicular from the track of the bow echo. The track of the bow echo is the path of its apex. The apex is the point on the convective line with greatest curvature and is subjectively determined from radar composites. Positive y-values are to the left and negative y-values to the right of the track, looking in the direction of motion (Fig. 2).

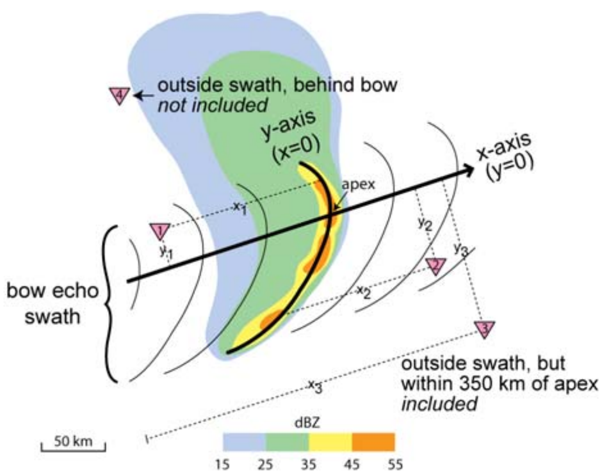

Fig. 2. Schematic reflectivity pattern for a bow echo with hypothetical positions of thermodynamic soundings (pink triangles with enclosed numbers). Soundings within the convective line swath (such as 1 and 2) are automatically included in the bow echo composite. Sounding 3 is also included, despite being outside the swath, since it precedes the convective line and is within 350 km of the apex. Sounding 4 is discarded because it is behind the convective line and outside the swath. Bow echo-relative coordinates (x_n, y_n) are proportional to the lengths of the perpendicular dashed lines shown emanating from the triangles. For sounding 3, since it is outside the bow echo swath, x-distance must be estimated by using an imaginary extension of the actual bow echo convective line.

2.3 Removing environmental mean

To obtain bow echo-relative winds, we first subtract the motion of the bow echo. This is allowed to vary over the course of the bow echo. The remaining wind vectors are then rotated by $-\varphi$, where φ is the angular difference between the bow echo motion vector and due east. In this manner, the positive x-axis always points in the direction of bow echo movement.

To obtain temperature, pressure, and mixing ratio perturbations associated with the composite bow echo, we subtract an environmental profile from each sounding. Individual soundings are first interpolated to every 50-m MSL and then the variables are averaged at each level. All soundings at least 20 km ahead of the convective line ($x > 20$ km) are used to obtain the environmental profile. Soundings closer to the line might intersect the bow echo cold pool, so we ignore them. Once the average profile is calculated, it is subtracted from each sounding. This is repeated for each intensive observation period or IOP.

2.4 Objective analysis

We use GEMPAK software (version 5.9) to perform a two-pass Barnes objective analysis (Barnes, 1964; Koch et al. 1983) of upper air data onto a 0.1 x 0.1 deg latitude-longitude grid centered on 0 deg N, 0 deg E. This analysis is performed at 32 vertical levels. Their vertical separation ranges from 150 m near the surface to 1000 m above 6 km MSL. Height above ground level (AGL) differs from height MSL due to topography variation across the BAMEX domain, but the standard deviation is relatively small (170 m). On average, the surface is 300 m MSL, and for simplicity, when we refer to height AGL, we have simply subtracted 300 m from height MSL.

2.5 System-relative sonde distribution

a)

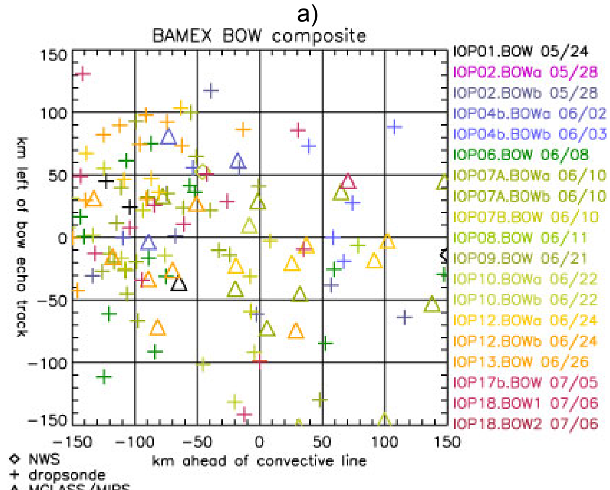

b)	Behind	Ahead	
Left	86	11	56%
Right	46	31	44%
	76%	24%	

Fig. 3. a) Sonde launch origins relative to bow echo apex (0, 0). In this coordinate system, x=0 represents the convective line, and bow echo motion is toward higher x. Locations beyond 150 km in x or y are omitted for clarity. Diamonds are NWS (and ARM), plus signs are dropsonde, and triangles are MGLASS launch locations. Symbols are color-coded by bow echo according to the legend on the right. Part b) summarizes the number of sondes by quadrant. These charts do not include the 204 locations of wind profiles from the NOAA Profiler Network (NPN)

The composite sounding distribution relative to the bow echo is not uniform (Fig. 3), but the density is adequate in most regions for an analysis. The only exception is the region ahead of the convective line to the far left of the bow echo apex (x>0km and y>100km) where no soundings were taken. Notably, only six out of the 174 soundings came from operational NWS balloons, which is a testament to the importance of BAMEX special field observations. Three out of four soundings (76%) were behind the convective line in a historically under-sampled region of the bow echo. Although the total number of dropsonde soundings far exceeds the surface-based soundings, a substantial fraction near the convective line is due to surface-based sondes. This is because MGLASS could launch close to the convective line in locations too risky for the Lear jet to fly.

3 BOW ECHO ENVIRONMENT

Soundings ahead of the bow echo show ample convective instability. For the 34 complete soundings at least 20 km ahead of the convective line, not touching the cold pool, the median value of CAPE is 1581 J kg^{-1} and the median lifted index (LI) is -5.7 K. The most unstable sounding has extreme values of 5858 J kg^{-1} and -16.3 K. To calculate CAPE and LI, we use virtual temperature and lift the low-level parcel with the highest theta-e. The complete histogram of environmental CAPE values is shown in Fig. 4. Although the instability is significant, it is not extremely high, as with the indices cited in previous studies based on derechos, severe wind producing storm complexes that are often made up of bow echoes (Johns and Hirt, 1987). This is probably because our sample is not limited to severe bow echoes and includes marginal bow echoes with less unstable environments.

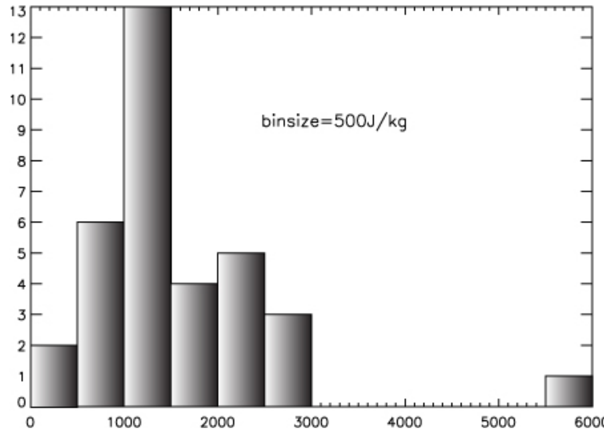

Fig. 4. Histogram of environmental CAPE values for composite bow echo.

Most of the soundings to the left of the bow echo track have a shallow temperature inversion near the surface, while the soundings to the right have a well-mixed surface layer. Reminiscent of the warm-season progressive derecho pattern described in Johns (1993), this suggests a weak thermal boundary is ahead of the bow echo and parallel to the bow echo motion vector. This is illustrated in a low-level horizontal cross section of temperature anomaly (Fig. 5).

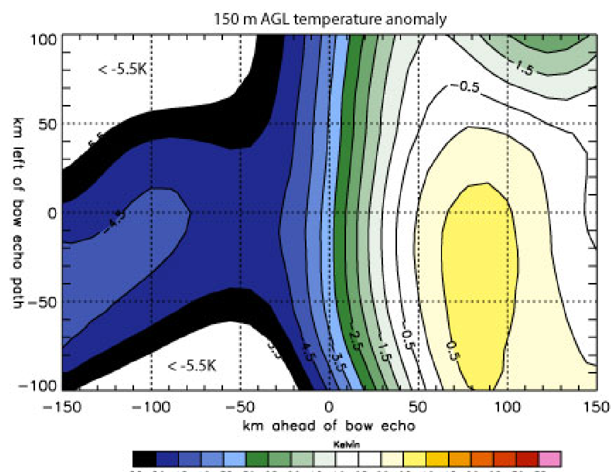

Fig. 5. Temperature anomaly at 150 m AGL. A strong cold pool (< -5 K) exists behind the convective line. Ahead of the line, there is a north-south temperature gradient. This gradient is apparent in cross sections up to 1 km AGL (not shown).

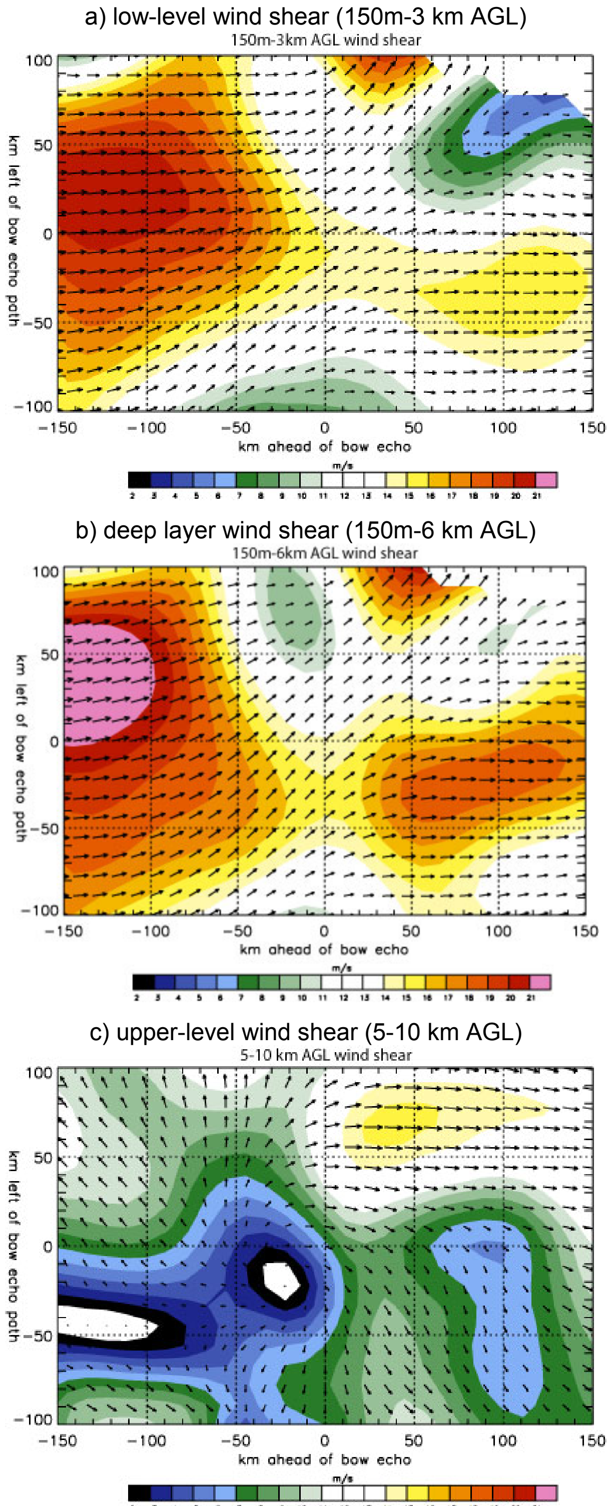

Fig. 6. Vertical wind shear vectors and magnitude (shaded; m s^{-1}) a) 150m-3km b) 150m-6 km and c) 5 km-10 km AGL.

Numerical studies have demonstrated the importance of low-level shear in maintaining strong updrafts along the leading edge of an advancing cold pool (Rotunno et al. 1998; Weisman 1993). The low-level and deep layer shear ahead of the composite bow echo (Fig. 6a, b) is consistent with these findings. For the low-level and deep wind shear, we select 150 m AGL as the lowest level because many soundings have no data below 150 m AGL. The shear vectors are oriented perpendicular to the convective line and enhanced along a narrow corridor that conveniently intersects the apex of the composite bow.

Observational studies have suggested it is not just the low-level shear that is vital for long-lived convective wind storms, but also the deep layer shear (Coniglio et al. 2004; Burke and Schultz 2004). Although the deep layer shear is greater than the low-level shear in the composite bow echo, much of the shear resides in the lower layer (150m-3km layer).

The deep layer wind shear vectors (Fig. 6b) show some evidence of partial thermal wind balance near the convective line. The counter-clockwise turning of the shear vectors may be in response to the baroclinic zone caused by the cold pool behind the bow echo.

Upper-level shear (5-10 km AGL; Fig. 6c) is relatively weak but not negligible. Recent numerical studies have shown that 5-10 m s^{-1} of shear in this layer can lift parcels to greater heights than identical environments without upper-level shear (Coniglio et al. 2006). The upper-level shear ahead of our composite bow echo is strongest in the forward left quadrant where values exceed 14 m s^{-1}. System-scale anti-cyclonic shear circumscribes the whole domain in response to sustained upper-level diabatic heating behind the convective line.

4 COMPOSITE BOW ECHO

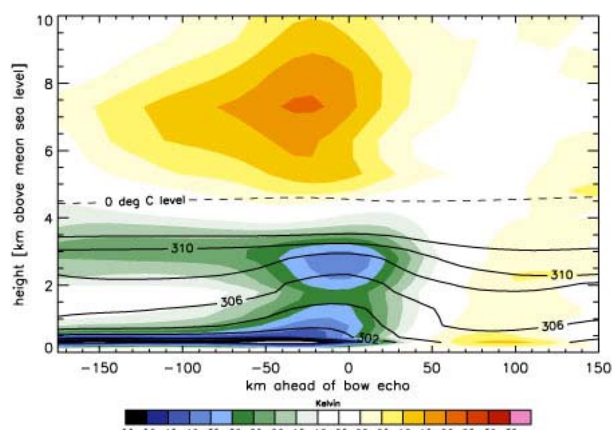

Fig. 7. Vertical cross section of temperature anomaly (shaded) through the bow echo apex along the path of the bow echo. Low-level potential temperature (Kelvin) contours are overlaid in black. A dashed line denotes the 0 deg C level.

The broad low-level temperature perturbation behind the convective line (Fig. 7) is essentially the bow echo cold pool. Assuming its depth is defined by the height of zero temperature perturbation, it extends about 4 km AGL, just below the 0 deg C level. The cold pool is strongest at the surface, with a secondary temperature minimum about 2-3 km AGL. The secondary minimum is likely maintained by melting and evaporation of stratiform precipitation into subsaturated air. This is hypothesis is consistent with the relative humidity cross section shown in Fig. 8. After precipitation is depleted, the downdrafts continue to warm dry-adiabatically, eroding the cold anomaly in a layer 1-2 km AGL. The subsiding air apparently cannot penetrate the very strong surface inversion.

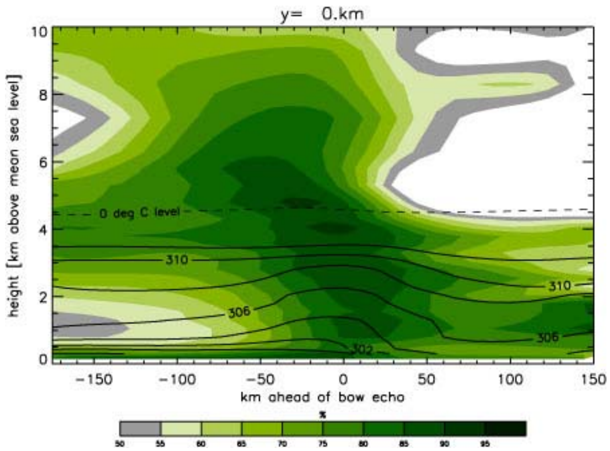

Fig. 8. Same as Fig. 7 but relative humidity.

The deep positive temperature perturbation aloft, just behind the convective line is from latent heat release within the convective and mesoscale updrafts.

Several authors (Fovell, 2002; Mapes, 1993; Nicholls et al; 1991) showed how low-frequency buoyancy waves from the parent MCS can propagate ahead of the system and destabilize the environment. Fovell (2002) simulated lower tropospheric changes of about 2 K and ~1 g kg^{-1} associated with these waves. These would be difficult to detect in our composite due to their small amplitude and due to destructive interference among waves at different locations relative to the convective line.

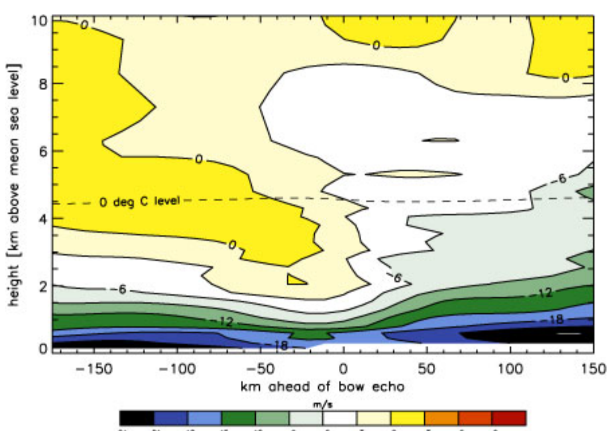

Fig. 9. Wind component perpendicular to the convective line.

One clearly sees the rear inflow jet (RIJ) in the cross section of bow echo–relative horizontal wind normal to the line (u; Fig. 9). From a maximum speed of ~3 m s^{-1} situated about 120-150 km behind the convective line, the RIJ slows and descends as it approaches the convective line. The enhanced flow associated with the RIJ projects towards the surface, but it is slower than the actual bow echo by the time it reaches the surface. The bow echo-relative values in the RIJ may appear low, but they are significant considering that the bow echo speeds (~20 m s^{-1}, on average) have already been subtracted. It is noteworthy that in their recent radar and damage analysis of severe BAMEX bow echoes Wheatley et al. (2006) found low-level mesovortices within the bows were responsible for the most damaging surface winds, not the descending rear inflow jet.

Weisman (1992) showed that an elevated rear inflow jet can help sustain erect updrafts ahead of a growing cold pool in a simulated mature bow echo. The tendency for the cold pool to overwhelm the environmental shear may be offset by the vertical shear beneath the elevated jet, allowing the system to persist in a quasi-balanced state. This may be what is happening in our bow echo composite, but there may also be some sampling issues near the surface along the convective line. Small-scale convective downdrafts near the convective line (with their attendant downward transfer of positive u momentum) are probably not resolved by our observation network.

The composite bow echo moves at about the same speed as the line-normal wind at 2-4 km elevation MSL just behind the line. Strong low level inflow is present in advance of the convective line.

5 SUMMARY

Using a high density soundings and wind profiles taken around and within bow echoes during BAMEX, a composite bow echo has been produced. Both kinematic and thermodynamic quantities are directly observed and assimilated into the composite.

The mean CAPE of soundings ahead of the bow echo is 1581 J kg^{-1}. A near-surface inversion is found in most soundings on the left side ahead of the bow echo, while the right side has predominantly well-mixed layers near the surface which is consistent with propagation along a low-level thermal boundary. There is strong storm-relative (20+ m s^{-1}) low-level inflow.

A deep cold pool is evident in the bow echo composite, with a negative temperature perturbation extending from the surface to 4 km AGL. The cold anomaly is strongest below 100 m AGL, with a secondary temperature minimum observed 2-3 km AGL.

Wind shear normal to the leading convective line is about 15 m s^{-1}, primarily below 3 km AGL. Moderate upper-level shear (5-10 km AGL) exists in the forward left quadrant ahead of the bow echo apex.

The composite rear inflow jet starts out near the melting level around 5 km AGL, 200 km behind the line and descends to 2 km AGL. It is not clear how it interacts with surface flow just behind the convective line.

It is important to note the composite is a mixture of several bow echoes and does not represent any particular event. Any particular event will have higher amplitude anomalies associated with it, since the averaging process will smooth out the peaks due to variation of storm structure among different events.

6 REFERENCES

Barnes, S. L., 1964: A technique for maximizing details in numerical weather map analysis. J. Appl. Meteor., 3, 396-409.

Burke P. C., D. M. Schultz. 2004. A 4-yr climatology of cold-season bow echoes over the continental United States. Wea. Forecasting. 19, 1061-1074.

Coniglio, M. C., D. J. Stensrud, L. J. Wicker, 2006: Effects of Upper-Level Shear on the Structure and Maintenance of Strong Quasi-Linear Mesoscale Convective Systems. J. Atmos. Sci. 63, 1231-1252.

Coniglio M. C., D. J. Stensrud, M. B. Richman, 2004. An observational study of derecho-producing convective systems. Wea. Forecasting. 19, 320-337.

Davis, C., N. Atkins, D. Bartels, L. Bosart, M. Coniglio, G. Bryan, W. Cotton, D. Dowell, B. Jewett, R. Johns, D. Jorgensen, J. Knievel, K. Knupp, W.-C. Lee, G. Mcfarquhar, J. Moore, R. Przybylinski, R. Rauber, B. Smull, R. Trapp, S. Trier, R. Wakimoto, M. Weisman, C. Ziegler, 2004: The Bow Echo and MCV Experiment: Observations and opportunities. Bull. Amer. Meteor. Soc., 85, 1075-1093.

Evans, J. S. and C. Doswell, 1991: Examination of derecho environments using proximity soundings. Wea. Forecasting, 16, 329.

Fovell, R. G., 2002: Upstream influence of numerically simulated squall-line storms. Q. J. Roy. Meteor. Soc., 128, 893-912.

FSL, cited 2006: Meaning of Low_qual_summary & High_qual_summary: (1998FEB26), NOAA Wind Profiler Quality Control Usage Note: 26 August 1996. [Available online at http://dss.ucar.edu/datasets/ds359.0/docs/QUALITY.CODE.19980226.]

Johns, R.H., 1993: Meteorological conditions associated with bow echo development in convective storms. Wea. For., 8, 294-299.

Johns, R. H., and W. D. Hirt, 1987: Derechos: Widespread convectively induced wind-storms. Wea. Forecasting, 2, 32-49.

JOSS, cited 2006: BAMEX Sounding Composite 5mb Level Upper Air Data [JOSS]. [Available online at http://www.joss.ucar.edu/data/bamex/docs/readme.bamex_5mb_interp_snd_comp.]

Klimowski, B. A., M. R. Hjelmfelt, and M. J. Bunkers, 2004: Radar observations of the early evolution of bow echoes. Wea. Forecasting, 19, 727-734.

Koch, S. E., M. desJardins and P. J. Kocin, 1983: An Interactive Barnes Objective Map Analysis Scheme for Use with Satellite and Conventional Data. J. Appl. Meteor., 22, 1487-1503.

Mapes, B. E., 1993: Gregarious Tropical Convection. J. Atmos. Sci., 50, 2026-2037.

Nicholls, M.E., R. A. Peilke, and W. R. Cotton, 1991: Thermally forced gravity-waves in an atmosphere at rest. J. Atmos. Sci., 48, 1869-1884.

Przybylinski, R. W., 1995: The bow echo: Observations, numerical simulations, and severe weather detection methods. Wea. Forecasting., 10, 203-218.

Rotunno, R., J. B. Klemp and M. L. Weisman, 1988: A theory for strong, long-lived squall lines. J. Atmos. Sci., 45, 463-485.

Weber, B.L., D.B. Wuertz, D.C. Welsh, and R. McPeek, 1993: Quality controls for profiler measurements of winds and RASS temperatures. J. Atmos. Oceanic Technol., 10, 452-464.

Weisman, M. L., 1992: The role of convectively generated rear-inflow jets in the evolution of long-lived mesoconvective systems. J. Atmos. Sci., 49, 1826-1847.

Weisman, M. L., 1993: The genesis of severe, long-lived bow echoes. J. Atmos. Sci., 50, 645-670.

Weisman, M. L. and C. A. Davis, 1998: Mechanisms for the generation of mesoscale vortices within quasi-linear convective systems. J. Atmos. Sci., 55, 2603-2622.

Wheatley, D. M., R. J. Trapp, and N. T. Atkins, 2006: Radar and Damage Analysis of Severe Bow Echoes Observed during BAMEX. Mon. Wea. Rev. 134, 791-806.